Mol Neurobiol (2012) 45:455–464
DOI 10.1007/s12035-012-8254-0

Anti-proliferative Effects of Tricyclodecan-9-yl-xanthogenate (D609) Involve Ceramide and Cell Cycle Inhibition

Anchal Gusain · James F. Hatcher · Rao Muralikrishna Adibhatla · Umadevi V. Wesley · Robert J. Dempsey

Received: 13 January 2012 / Accepted: 1 March 2012 / Published online: 14 March 2012

Abstract Tricyclodecan-9-yl-xanthogenate (D609) inhibits phosphatidylcholine (PC)-phospholipase C (PLC) and/or sphingomyelin (SM) synthase (SMS). Inhibiting SMS can increase ceramide levels, which can inhibit cell proliferation. Here, we examined how individual inflammatory and glia cell proliferation is altered by D609. Treatment with 100-μM D609 significantly attenuated the proliferation of RAW 264.7 macrophages, N9 and BV-2 microglia, and $DITNC_1$ astrocytes, without affecting cell viability. D609 significantly inhibited BrdU incorporation in BV-2 microglia and caused accumulation of cells in G_1 phase with decreased number of cells in the S phase. D609 treatment for 2 h significantly increased ceramide levels in BV-2 microglia, which, following a media change, returned to control levels 22 h later. This suggests that the effect of D609 may be mediated, at least in part, through ceramide increase via SMS inhibition. Western blots demonstrated that 2-h treatment of BV-2 microglia with D609 increased expression of the cyclin-dependent kinase (Cdk) inhibitor p21 and down-regulated phospho-retinoblastoma (Rb), both of which returned to basal levels 22 h after removal of D609. Exogenous C8-ceramide also inhibited BV-2 microglia proliferation without loss of viability and decreased BrdU incorporation, supporting the involvement of ceramide in D609-mediated cell cycle arrest. Our current data suggest that D609 may offer benefit after stroke (Adibhatla and Hatcher, *Mol Neurobiol* 41:206–217, 2010) through ceramide-mediated cell cycle arrest, thus restricting glial cell proliferation.

Keywords Astrocytes · BrdU · Cell cycle · Ceramide · Flow cytometry · Macrophages · Microglia · p21 · Sphingomyelin synthase

Anchal Gusain and James F. Hatcher contributed equally to this manuscript.

A. Gusain · J. F. Hatcher · R. M. Adibhatla (✉) · U. V. Wesley · R. J. Dempsey (✉)
Department of Neurological Surgery,
School of Medicine and Public Health, University of Wisconsin,
Box 8660, Clinical Science Center, 600 Highland Ave,
Madison, WI 53792, USA
e-mail: adibhatl@neurosurg.wisc.edu
e-mail: dempsey@neurosurg.wisc.edu

R. M. Adibhatla
Cardiovascular Research Center,
School of Medicine and Public Health, University of Wisconsin,
Madison, WI, USA

R. M. Adibhatla
Neuroscience Training Program,
School of Medicine and Public Health, University of Wisconsin,
Madison, WI, USA

A. Gusain · J. F. Hatcher · R. M. Adibhatla · R. J. Dempsey
William S. Middleton Veterans Affairs Hospital,
Madison, WI, USA

Introduction

Xanthates including tricyclodecan-9-yl-xanthogenate (D609) were initially developed as broad spectrum antiviral compounds [1, 2]. D609 also has antioxidant properties [3, 4] due to the presence of the thiol function. D609 was shown to be a competitive inhibitor of bacterial phosphatidylcholine (PC)- specific phospholipase C (PC-PLC) and did not inhibit bacterial phosphatidylinositol-PLC, bovine pancreatic PLA_2, or phospholipase D from cabbage [5]. Many of the actions of D609 have been attributed to PC-PLC inhibition, including suppressing expression of hypoxia-inducible factor 1α after stroke [6], reduced cytokine expression in lipopolysaccharide (LPS)-stimulated

macrophages [7, 8], prevention of tumor necrosis factor-α, or LPS-induced lethal shock in mice [9]. A number of studies implicated PC-PLC in proliferation, differentiation, senescence, and apoptosis in mammalian cells as well as a role in atherosclerosis [10] and indirectly in stroke models [6, 11, 12]. A review of the literature on D609 various mechanisms of action was recently published [1].

Cell proliferation and growth arrest are regulated by two lipid second messengers with opposing actions [13]: ceramide and 1,2-diacylglycerol (DAG) that are connected through sphingomyelin (SM) synthase (SMS) pathway [14]. SMS transfers the phosphocholine group from PC to ceramide to form SM and DAG. There are two forms of SMS: SMS1 is located in the Golgi apparatus, and SMS2 is in the plasma membrane [15]. D609 inhibits both forms of SMS [16–18]. Inhibition of SMS can result in increased ceramide levels by blocking its incorporation into SM. D609 inhibited bFGF-stimulated astrocyte proliferation, which was attributed to SMS inhibition [19].

After cerebral ischemia, proliferation of astrocytes and microglia contributes to glial scar formation and release of inflammatory factors [20]. Cell proliferation is a precisely regulated process governed largely by cyclin-dependent kinases (Cdks) and their respective cyclin binding proteins. In the G_1 phase of the cell cycle, Cdk4 and Cdk6 bind to and are activated by D-type cyclins and initiate phosphorylation of retinoblastoma (Rb) protein, releasing E2F transcription factors for transcription of genes required for cell cycle progression. Subsequently, Cdk2 binds to and is activated by cyclin E, completing phosphorylation of Rb, allowing further E2F transcription and progression into the S-phase of DNA replication [21]. Activities of Cdk/cyclin complexes and cell cycle progression are regulated by two classes of Cdk inhibitors, the INK4 family and the Cip/Kip family $p21^{CIP1/WAF1}$, $p27^{Kip1}$, and $p57^{Kip2}$. Ceramide can inhibit proliferation by up-regulating the Cdk inhibitors p21 and p27 or de-phosphorylating Rb [22].

Our previous studies showed that D609 decreased infarct in an in vivo stroke model and up-regulated p21 [23]. In this study, we show that D609 inhibited proliferation of non-neuronal cell lines without inducing cell death. D609 treatment increased ceramide levels and up-regulated p21 expression in BV-2 microglia. In addition, D609 hypophosphorylated Rb, resulting in inhibition of the cell cycle in the G_0/G_1 phase and a decrease in the proportion of cells in the S-phase. Exogenous C8-ceramide studies support the involvement of ceramide in D609-mediated cell cycle arrest.

Materials and Methods

All chemicals and reagents unless stated otherwise were purchased from Sigma (St. Louis, MO). D609 was obtained from Kamiya Biomedical Company (Seattle, WA). The following antibodies were obtained from the indicated suppliers: p21 (BD Biosciences, San Diego, CA), phospho-Rb (Ser807/811) (Cell Signaling, Danvers, MA), and horseradish peroxidase conjugated goat anti-rabbit and goat anti-mouse IgG (Bio-Rad, Hercules, CA). Western blot detection used SuperSignal West Pico chemiluminescent reagent (Pierce, Rockford, IL).

Cell Culture

The murine BV-2 microglia cell line developed by Dr. V. Bocchini [24] was a generous gift from Dr. Grace Y Sun (University of Missouri, Columbia, MO). Murine N9 microglial cells, originally developed by Prof. P. Ricciardi-Castagnoli [25], were kindly provided by Dr. Jyoti Watters (University of Wisconsin, Madison, WI). RAW 264.7 [26] and $DITNC_1$ [27] were procured from American Type Culture Collection (ATCC, Manassas, VA). All the cell lines were maintained in DMEM/high glucose containing 10 % FBS with 100-U/mL penicillin and 100-μg/mL streptomycin. For all the experiments, cells were plated and allowed to attach overnight, and specific treatments were given the next day. D609 was dissolved in sterile saline and added to cell cultures to give the desired concentration. D609 was stable in saline and cell culture media as measured by absorption maximum at 300 nm [28], and <10 % decrease in absorption was observed after 24 h (personal communication, H Kalluri) unlike the short half life previously reported [29]. We also did not observe any absorption at 350 nm indicative of disulfide formation over 24 h [28]. C8-ceramide dissolved in 100 % EtOH was first dispersed in a small volume of media by gentle vortexing and then added to cultures of BV-2. There are two reasons of using C8-ceramide in our studies: (1) The structure of C2-ceramide is more like that of sphingosine than ceramides [30], and (2) C8-ceramide is also cell-permeable, and its levels in treated cells and media could be analyzed using our existing GC method. Hexane used as solvent carrier for GC will mask the methyl esters derived from C2-or C6-ceramides.

Western Blotting

Cells were lysed in protein extraction buffer consisting of 20-mM Na_2HPO_4, 50-mM NaF, 10-mM $Na_4P_2O_7$, 150-mM NaCl, 5-mM EGTA, 5-mM EDTA, 2 % Triton X-100, and 0.5 % deoxycholate; Na_3VO_4 (1 mM) and Sigma protease inhibitor cocktail were added to the extraction buffer immediately prior to use. Cell lysates were briefly sonicated and centrifuged at 13,000 rpm for 10 min at 4°C. Supernatant was used for protein estimation by Lowry's method. Fifty micrograms of protein was loaded in each well of 10 % or 12 % polyacrylamide gels and subjected to SDS-PAGE at a constant voltage of 150 V. Proteins were subsequently transferred to nitrocellulose at a constant voltage of 100 V for

1 h. Non-specific binding sites were blocked with 5 % non-fat dry milk in 1× Tris buffered saline (TBS) with 0.05 % Tween-20 (1× TBST) at room temperature for 1 h. Blots were incubated with primary antibodies (diluted in either 5 % BSA or 5 % non-fat dry milk in 1× TBST) for overnight at 4°C, washed with 1× TBST, and then incubated with appropriate secondary antibodies for 1 h at room temperature. After washing, protein bands were visualized with SuperSignal West Pico. Blots were subsequently stripped and reprobed for β-actin as a loading control.

BrdU Labeling

BV-2 microglia were plated in 96 well plates at a density of 2×10^4 cells per well. Cells were treated with 100-μM D609 for 2 h or 30-μM C8-ceramide for 2, 4, and 6 h. Chase was done with 5-μM BrdU at 37°C for 2 h, followed by fixation in ice cold methanol for 10 min. DNA was denatured with 2 N HCl for 30 min. Cells were washed four times with 1× PBS after each step. Non-specific sites were blocked with 10 % normal donkey serum in 0.5 % BSA and 0.4 % Triton-X100 for 45 min at RT. Cells were incubated with anti-BrdU primary antibody (1:50, Invitrogen) overnight at 4°C. After four washings, cells were probed with Alexafluor-488 conjugated donkey anti-mouse (1:500, Molecular Probes) for 1 h. Nuclei were counter-stained with DAPI (10 μg/mL). Images were acquired with a Nikon TE300 epifluorescence microscope and then analyzed using ImageJ (public domain software available at http://rsbweb.nih.gov/ij/); results were expressed as the percentage of BrdU-positive nuclei.

Cell Cycle Analysis

Cell cycle analysis was carried out as described by Yang et al. [31]. BV-2 cells were plated and allowed to attach overnight. After D609 treatment, cells were washed with PBS and trypsinized. Cells were pelleted and adjusted to a concentration of 1–2×10^6 cells/mL. Cells were fixed by adding 3 mL of 100 % ethanol drop-wise into 1 mL of cell suspension with continuous vortexing. After fixation overnight at −20°C, cells were pelleted and resuspended gently in PBS with 1 % BSA. After two washes, cells were suspended in propidium iodide (PI) staining solution (50-μg/mL PI, 1-mg/mL RNase, 0.5 % triton-X) for 30 min at 37°C in the dark, and the cell cycle was analyzed using a flow cytometer (BD Biosciences, FACSCalibur). Data were analyzed using MODFIT cell cycle analysis program.

Lipid Analysis

Cell pellets were resuspended in 0.5-mL saline, and an aliquot was taken for protein measurement. The cell suspension was transferred into 3 mL of $CHCl_3$:MeOH 1:2, followed by additional saline and $CHCl_3$ [23]. The $CHCl_3$ layer containing the lipid extract was evaporated under a stream of nitrogen and redissolved in a small volume of $CHCl_3$:MeOH 9:1. Ceramide was separated on silica gel H plates (Analtech) developed in $CHCl_3$:MeOH:CH_3COOH (94:2:5). SM was separated on Whatman LK-5 silica gel plates using $CHCl_3$:EtOH:Et_3N:H_2O (30:35:35:7). Lipids were identified using authentic standards. DAG was separated on silica gel G plates (Analtech) using petroleum ether:diethyl ether:acetic acid (80:20:1 v/v/v) [11]. DAG, ceramide and SM bands were then scraped into 1.5-mL MeOH containing 30 μL of H_2SO_4 and 10 nmol of heptadecanoic acid (17:0) as an internal standard. SM and ceramide were methylated by heating at 100°C for 2 h , DAG was methylated by heating at 70°C for 30 min [11, 23]. Fatty acid methyl esters were extracted into hexane and analyzed by gas chromatography. For analysis of C8-ceramide in media, 0.5-mL aliquots of media were extracted, and C8-ceramide was separated on silica gel H plates and analyzed by gas chromatography as discussed previously.

Statistical Analyses

Data were analyzed by ANOVA, followed by Bonferroni post-test for comparison of three or more groups or by non-paired *t*-test for comparison between two groups. A p value of 0.05 or less was taken as significant.

Results

Lower Doses and Shorter Durations of D609 Treatment Did Not Induce Caspase-3 Activation

The goal of our experiments was to determine if D609 could inhibit cell proliferation without inducing apoptosis or cell death. D609 has been shown to induce apoptosis dependent on the dose and duration of exposure [32]. BV-2 microglia treated with 50- or 100-μM D609 for 2 h followed by 22 h in media without D609 appeared morphologically normal and showed no significant trypan blue staining, whereas at 200 μM, many cells appeared shrunken and stained. Western blots were then conducted for pro-caspase-3 cleavage as a marker for induction of the apoptotic pathway [33]. Treatment of BV-2 with 50- or 100-μM D609 caused no detectable cleavage of caspase-3, whereas 200-μM D609 resulted in caspase-3 activation, indicating induction of apoptosis (Fig. 1a).

The time-course of D609 exposure on activation of caspase-3 was also investigated. BV-2 cells were treated with 100-μM D609 since 200 μM for 2 h induced apoptosis and preliminary findings indicated that 50 μM had no effect on cell numbers compared with controls 22 h after treatment. Exposure of BV-2 to 100-μM D609 for 2 h did not result in any detectable caspase-3 cleavage, whereas

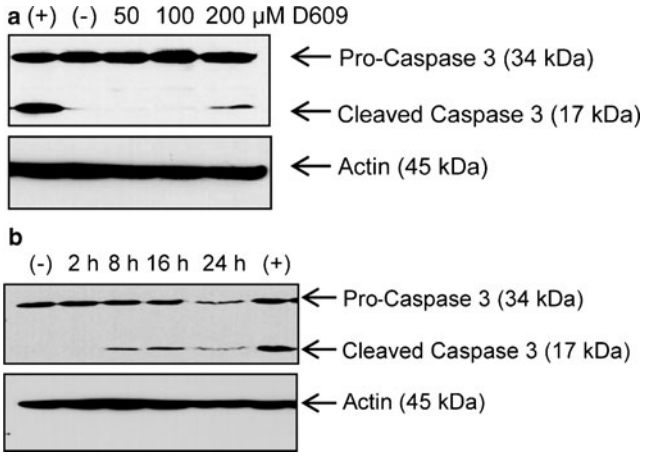

Fig. 1 D609 activates caspase-3 in a dose- and time-dependent manner. BV-2 cells treated with 20-μM etoposide for 24 h were used as a positive control for caspase-3 activation [53, 54]. **a** Western blot showing dose-response for D609 treatment of BV-2 cells for induction of cleaved caspase-3. Cells were incubated with 50-, 100-, and 200-μM D609 for 2 h, media were changed to remove D609, and cells were harvested after incubation for additional 22 h. Controls were incubated without D609. Lanes: (1) positive control (+), (2) untreated control (-), (3) 50-μM D609, (4) 100-μM D609, and (5) 200-μM D609. **b** Western blot showing effect of different treatment durations of BV-2 with 100-μM D609 on caspase-3 cleavage. BV-2 cells were treated with 100-μM D609 for 2, 8, 16, and 24 h and harvested at the end of each respective treatment time. Lanes: (1) untreated control (-), (2) 2-h D609, (3) 8-h D609, (4) 16-h D609, (5) 24-h D609, and (6) positive control (+)

exposure for 8 h or longer induced caspase-3 activation (Fig. 1b). The results in Fig. 1a, b demonstrate that 100-μM D609 for 2 h did not result in caspase-3 activation immediately following the treatment, and there was no delayed induction following 2-h treatment and 22 h in media without D609.

D609 Inhibited Proliferation of Various Cell Lines

The effect of D609 on proliferation of RAW 264.7 macrophages, BV-2 and N9 microglia, and $DITNC_1$ astrocytes was investigated. D609 significantly inhibited proliferation of all four cell lines (Fig. 2) without causing cell death, as viability remained >90 % by trypan blue exclusion in all cases. These data demonstrate that the inhibitory effect of D609 on cell proliferation is not unique to a particular cell line and also suggest that D609 may inhibit the cell cycle.

D609 Inhibited BrdU Incorporation and Caused Cell Cycle Arrest in G_0/G_1 Phase

To assess the effect of D609 on the cell cycle, further studies were conducted using the BV-2 cell line. BV-2 was treated with 100-μM D609 for 2 h, followed by a 2-h incubation with BrdU without D609. Two sets of images were captured from four wells each from controls and D609 treated. Representative images are presented in Fig. 3a, and results are presented as the percentage of BrdU-positive cells (Fig. 3b). D609 treatment significantly decreased the percent of BrdU-positive cells, indicating fewer cells progressing into the S-phase of the cell cycle.

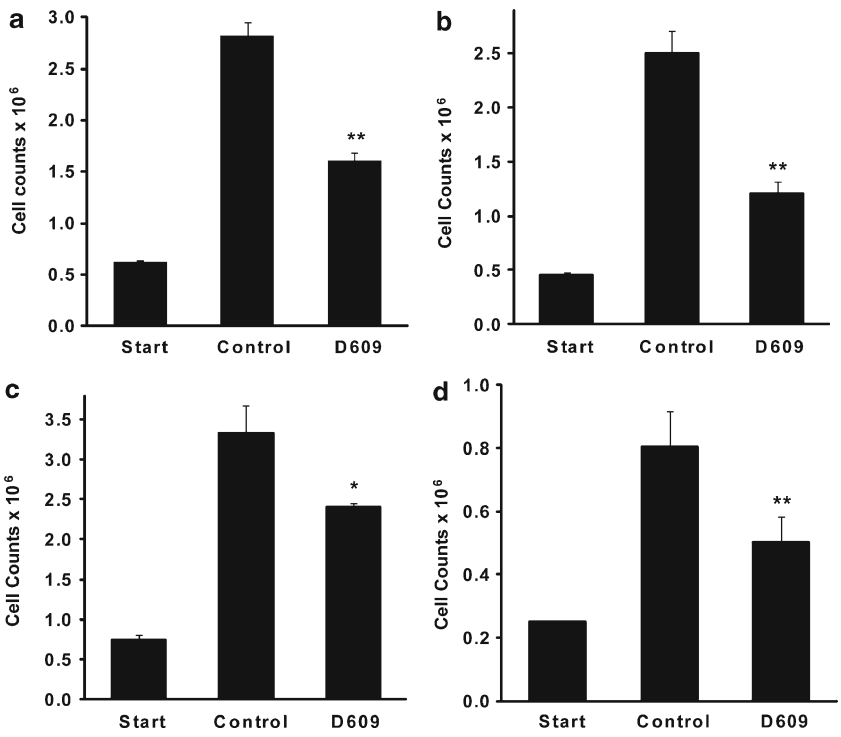

Fig. 2 D609 inhibited proliferation of **a** BV-2 microglia, **b** N9 microglia, **c** RAW 264.7 macrophages, and **d** $DITNC_1$ astrocytes. Cell lines were first plated and allowed to adhere overnight. At the start of treatment, parallel dishes of cells were harvested and counted to determine the initial cell number. Cells were treated with 100-μM D609 for 2 h, followed by a media change. The media were centrifuged to recover any non-adherent cells, which were returned to the respective dishes. Cells were counted using a hemocytometer, and viability was determined by trypan blue exclusion following 22-h incubation without D609. Viability was greater than 90 % in all cells. $^{*}p<0.05$ and $^{**}p<0.01$ compared with controls by unpaired *t*-test ($n=3$/group)

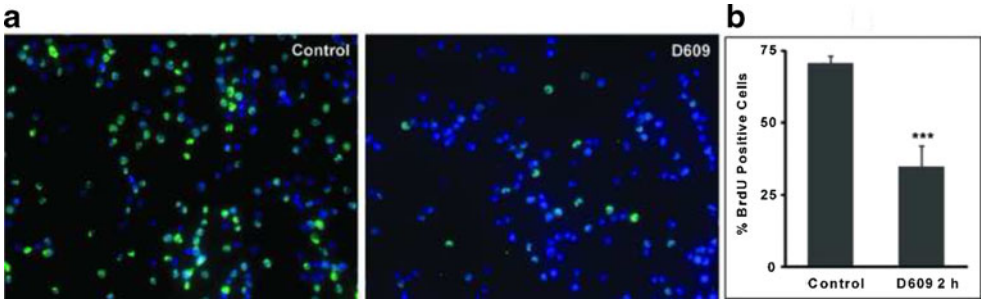

Fig. 3 D609 inhibited BrdU incorporation in BV-2 cells. **a** BrdU uptake in BV-2 controls and cells treated with D609. Cells were plated in 96-well plates, allowed to attach overnight, and then treated with 100-μM D609 for 2 h. The media were then replaced with fresh media containing BrdU, and cells were incubated for 2 h. Cells were labeled with anti-BrdU antibody, followed by DAPI counterstaining, and imaged. *Blue* DAPI, *green* BrdU. Original magnification×200. **b** Quantification of BrdU-positive cells as a percentage of total cells. $^{***}p<0.001$ compared with controls by unpaired *t*-test. Note: Figs. 3 and 7 may appear black and white in print version

Based on the BrdU uptake studies, cell cycle analysis was done in BV-2 by flow cytometric analysis of PI staining. After 2-h D609 treatment followed by 2 h in media without D609, the percentage of the BV-2 cells in the G_1 phase increased (54.3±1.5 %) as compared with the control (43.4±3.9 %), whereas the percentage of cells in the S phase showed a significant dip (39.9±3.3 %) as compared with control (48.8±2.4 %) (Fig. 4). No significant change in the proportion of cells in each cell cycle phase was found following D609 exposure for 2 h alone (data not shown).

D609 Increased Ceramide Levels and Altered Expression of Cell Cycle Proteins

Since D609 inhibits SMS, which could cause cellular ceramide levels to increase and possibly to decrease DAG levels, ceramide levels were measured in BV-2 cells treated with 100-μM D609 for 2 h and following a media change and further incubation without D609 for an additional 2 and 22 h. These conditions corresponded with treatment of BV-2 with D609 for cell proliferation by cell counts and BrdU incorporation. Ceramide levels were normalized to protein content, and the results are presented in Fig. 5a. Ceramides in BV-2 cells contained primarily the fatty acids palmitic (16:0), lignoceric (24:0), and nervonic (24:1); results are given for the sum of these three forms. D609 treatment for 2 h resulted in a significant increase in ceramide levels, which remained elevated for 2 h after removal of the agent. Following further incubation for 22 h without D609, ceramide levels returned to control levels. These results show that D609 treatment of BV-2 cells caused a transient, reversible increase in ceramide. Under these same treatment conditions, D609 did not cause DAG levels to decrease, but instead, a significant increase was observed (Table 1).

The increase in ceramide by D609 prompted us to examine whether D609 could increase expression of the Cdk inhibitor p21 and down-regulate phosphorylation of Rb (phospho-Rb). BV-2 cells were treated, as discussed previously, with 100-μM D609 and harvested after 2-h exposure and following 2- and 22-h incubation without the agent and processed for Western blotting. In parallel with the increase in ceramide, D609 treatment for 2 h up-regulated p21 expression and caused a decrease in phospho-Rb (Fig. 5b), consistent with

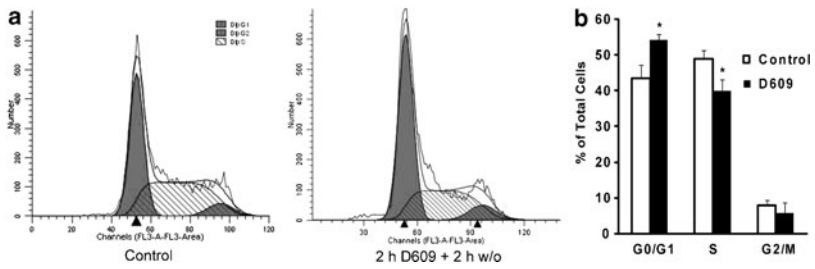

Fig. 4 Effect of D609 treatment on cell cycle progression in BV-2 cells. **a** Representative DNA histogram from control and D609 treatment groups. BV-2 cells were treated with 100-μM D609 for 2 h, followed by 2 h in media without D609, and then stained with propidium iodide. DNA content of the samples was analyzed by flow cytometry. **b** Quantification of the percentage of cells in each phase of cell cycle. A 2-h D609 followed by 2 h in the media without D609 has arrested the cells in the G_1 phase with a smaller percentage of cells entering into the S phase. $^{*}p<0.05$ compared with controls by unpaired *t*-test, from three independent experiments

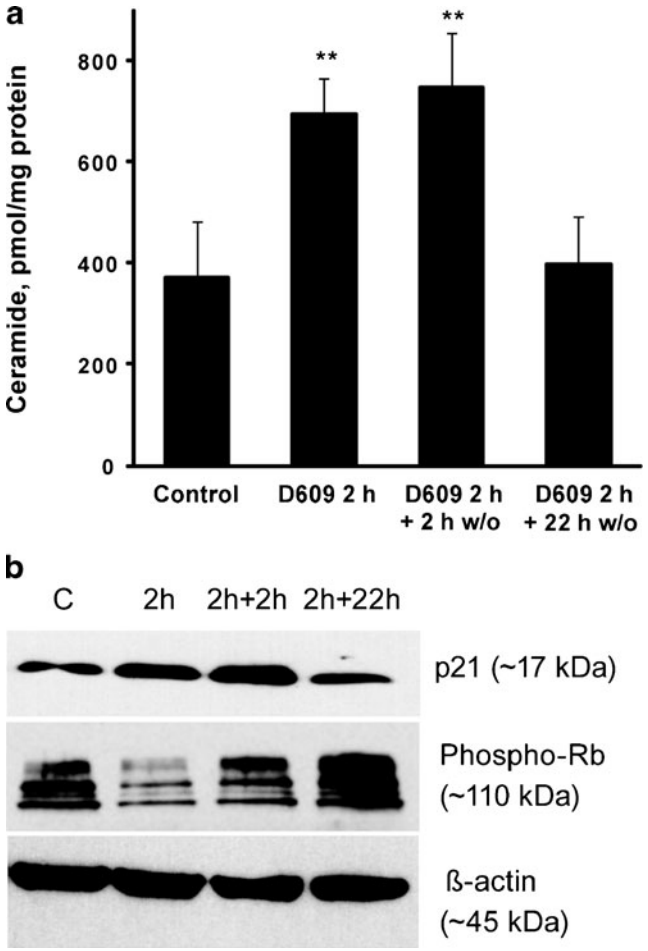

Fig. 5 D609 increased ceramide levels and induced p21 expression in BV-2 cells. BV-2 cells were treated with 100-μM D609 for 2 h, the media were changed, and cultures were incubated for an additional 2 or 22 h without D609. **a** D609 increased ceramide levels in BV-2, which remained elevated for 2 h after removal of the agent and normalized to control levels after 22 h. $^{**}p<0.01$ compared with controls or D609 2 h +22 h w/o by ANOVA with Bonferroni's post-test; $n=4$ per group from two independent experiments. Ceramide forms consisted mainly of palmitic (C16-ceramide), lignoceric (C24-ceramide), and nervonic (C24:1-ceramide). **b** Western blots demonstrating induction of p21 and down-regulation of pRb following D609 treatment. Lanes: (1) untreated control, (2) 100-μM D609 2 h, (3) 100-μM D609 2 h+2 h w/o, and (4) 100-μM D609 2 h+22 h w/o

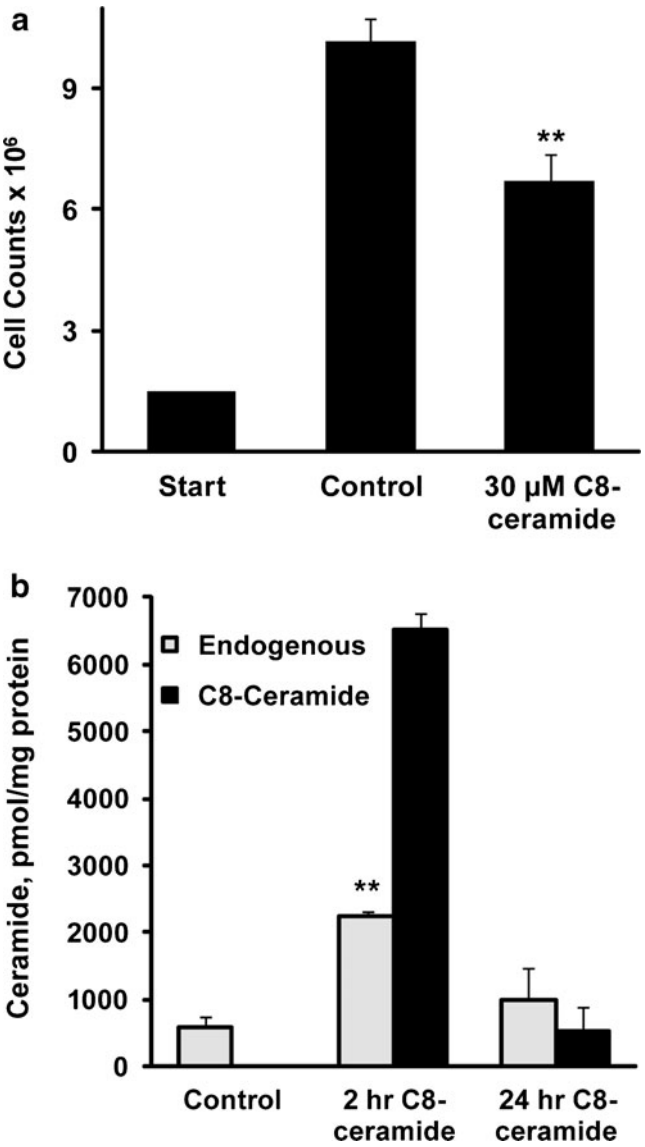

Fig. 6 Exogenous C8-ceramide decreased cell proliferation in BV-2 cells. **a** 30-μM C8-ceramide was added to BV-2 cultures, and cell counts and viability were determined after 24 h. $^{**}p<0.01$ compared with controls by unpaired *t*-test. **b** Uptake of C8-ceramide and endogenous ceramide levels in BV-2 after 2- and 24-h treatment with 30-μM C8-ceramide. $^{**}p<0.01$ compared with controls by ANOVA with Bonferroni's post-test

inhibition of the cell cycle. These alterations normalized to control levels 22 h after removal of the agent (Fig. 5b), indicating that the cells have returned to a proliferative state.

Table 1 DAG levels (nmol/mg protein, 2 fatty acids per DAG; primarily 16:0; 18:0; 18:1; 18:2, 20:4 minor) in BV-2 treated with 100-μM D609

Control ($n=5$)	2-h D609 ($n=5$)	2-h D609/2 h ($n=4$)	2-h D609/24 h ($n=4$)
1.77±0.17	2.14±0.08*	2.25±0.14*	2.18±0.32*

* $p<0.05$ compared to control

Exogenous C8-ceramide: Effect on Cell Proliferation, Viability, and Cellular Uptake

To determine the specific role of ceramide in D609-mediated inhibition of proliferation, BV-2 cells were treated with varying concentrations of cell-permeable C8-ceramide [34]. Cell counts and viability were determined after 24 h. Treatment of BV-2 cells with 30-μM C8-ceramide for 24 h significantly inhibited proliferation (Fig. 6a) without inducing cell death (viability: controls 94±0.2 % vs C8-ceramide 93±0.5 %, $n=3$ each). Treatment with 20-μM C8-ceramide had no

Table 2 Individual and total ceramide levels (nmol/mg protein) in BV-2 treated with 30-μM C8-ceramide

	8:0	16:0	24:0	24:1	Total
Control (n=6)	0	0.25±0.07	0.23±0.05	0.11±0.04	0.59±0.15
2 h (n=3)	6.53±0.25	1.31±0.06	0.55±0.0 3	0.38±0.01	8.77±0.32
24 h (n=3)	0.52±0.36	0.42±0.30	0.37±0.13	0.19±0.05	1.50±0.83

significant effect on proliferation, whereas 40 μM resulted in significant cell death (data not shown). Based on these results, 30-μM C8-ceramide was used for treatment of BV-2 cells in further studies.

Cellular ceramide levels were analyzed following 2- and 24-h exposure to 30-μM C8-ceramide to determine uptake by BV-2 cells (Table 2). Following 2-h incubation, C8-ceramide levels had reached 6,529±245 pmol/mg protein, demonstrating substantial uptake (Fig. 6b). No C8-ceramide was detected in untreated cells. Interestingly, the endogenous forms of ceramide comprised of 16:0, 24:0, and 24:1 fatty acids also showed significant increases (Fig. 6b). Following 24-h exposure to C8-ceramide, cellular levels of C8-ceramide had declined to <10 % of the 2-h levels. The endogenous forms had also declined to less than half the 2-h levels and were not significantly elevated above controls (Fig. 6b).

Treatment of BV-2 with C8-ceramide resulted in a small but not significant increase in SM due to incorporation of C8-ceramide (controls 8.17±0.40 vs 2-h C8-ceramide 9.36± 0.07 nmol/mg protein, n=3 each). SM in normal BV-2 was composed of 16:0, 24:0, and 24:1 fatty acids. After 2 h, incorporation of C8-ceramide into SM accounted for 16.4±0.2 % of total fatty acids of SM. At 24 h, SM levels were 8.94± 0.58 nmol/mg protein in BV-2 treated with C8-ceramide, and the C8 content of SM had declined to 10.5±2.8 % (Table 3).

Towards gaining insight onto the decline in ceramide levels in BV-2 exposed to C8-ceramide for 24 h, C8-ceramide levels in media from treated BV-2 cells were analyzed and found to have declined to <1 μM by 24 h (Table 4). As a stability control, 30-μM C8-ceramide was added to control media and incubated at 37°C without cells. C8-ceramide levels remained constant for up to 24 h (Table 4), demonstrating that there was no decomposition.

Exogenous C8-ceramide Inhibited BrdU Uptake

To further assess the mechanism of exogenous C8-ceramide mediated inhibition of cell proliferation, BV-2 cells were treated with 30-μm C8-ceramide for 2, 4, and 6 h, followed by 2-h BrdU chase without C8-ceramide. Representative images are presented in Fig. 7a, and the results are presented as the percentage of BrdU-positive cells (Fig. 7b). C8-ceramide treatment for 2 or 4 h did not significantly decrease the percent of BrdU positive cells compared to controls (data not shown), whereas BrdU incorporation was significantly inhibited by 6-h C8-ceramide treatment, indicating fewer cells entering the S phase.

Discussion

Our previous findings in an in vivo stroke model showed that D609 treatment up-regulated the Cdk inhibitor p21 [23]. Since ceramide can up-regulate p21 [22], we hypothesized that D609 increased p21 expression through inhibition of SMS and increased ceramide levels, and that this would result in cell cycle inhibition. We therefore examined the effect of D609 on proliferation of microglia, macrophage, and astrocyte cell lines. Since ceramide also induces apoptosis [35, 36], we considered that over-induction of ceramide accumulation by D609 would result in cell death but that moderate increases may cause growth arrest without affecting cell viability.

Utilizing the BV-2 microglia cell line, our studies showed that D609 could cause caspase-3 cleavage, indicative of apoptosis, or inhibit cell proliferation without causing cell death and that inhibition of the cell cycle vs induction of apoptosis was dependent on the dose and duration of exposure. These data are consistent with previous reports demonstrating that D609 treatment of bFGF-stimulated neural stem cells for 1 to 3 days induced apoptosis [32]. In other studies, a shorter 4-h exposure to D609 inhibited [^{3}H]-thymidine uptake in bFGF-stimulated astrocytes [19]. Our results showed that D609 could inhibit proliferation of microglia, macrophage, and astrocyte cell lines, indicating that this effect is not unique to a specific cell line. However, previous studies have not examined the effect of D609 on

Table 3 Individual and total sphingomyelin levels (nmol/mg protein) in BV-2 treated with 30-μM C8-ceramide

	8:0	16:0	24:0	24:1	Total
Control (n=3)	0	5.01±0.25	1.54±0.10	1.62±0.06	8.17±0.40
2 h (n=3)	1.54±0.02	4.62±0.04	1.42±0.01	1.78±0.04	9.36±0.07
24 h (n=3)	0.95±0.31	5.22±0.13	1.33±0.06	1.44±0.10	8.94±0.58

Table 4 C8-ceramide levels (μM) in culture media after adding to media at 30 μM

	0 h	2 h	8 h	24 h
Media alone (n=2)	27.5±0.17	26.3±0.01	27.6±0.16	31.1±3.5
Media from BV-2 (n=3)	–	16.3±1.3	–	0.7±0.3

expression of cell cycle regulating proteins. Utilizing the BV-2 microglia cell line, our studies demonstrated that D609 increased ceramide levels and induced expression of cyclin/Cdk inhibitory protein p21, resulting in a decrease in cells in the S- and G_2/M phases due to a block in the cell cycle in G_0/G_1. Interestingly, D609 treatment did not cause a decrease in levels of DAG that is classically associated with cell proliferation [13], but rather a significant increase was observed (Table 1), supporting the role of ceramide in anti-proliferative effects. The increase in DAG might represent a cellular response to maintain homeostasis [14]. On an average, the lipid levels (nmol/mg protein) in BV-2 microglia cells are PC 35–45, SM 7.5–9, and DAG 2–2.5, while ceramide levels are <0.5. Since the levels of ceramide are a small fraction of PC, SM, and DAG, observing changes in these lipid pools due to SMS inhibition might be masked. Treatment of BV-2 cells with exogenous C8-ceramide also inhibited cell proliferation and BrdU incorporation, supporting the role of ceramide in D609-mediated inhibition of cell proliferation. The effect of D609 on proliferation of BV-2 microglia appeared to be more robust than treatment with exogenous C8-ceramide. Since ceramide is highly hydrophobic, it generally resides in cellular membranes, and its effects are strongly influenced by cellular compartmentalization [37]. Exogenous short-chain ceramides are transported to the Golgi apparatus following cellular uptake [38, 39]. D609 inhibition of both forms of SMS [16–18] could result in ceramide increases in both Golgi apparatus and plasma membrane due to the sub-cellular localizations of SMS1 (Golgi apparatus) and SMS2 (plasma membrane) [15]. C8-ceramide was incorporated into sphingomyelin demonstrated by formation of C8-SM (Table 3), evidence that some of C8-ceramide reached the pool used by SMS. The effects of ceramide sub-cellular distribution in its signaling remain an important topic for future exploration.

Incubation of BV-2 with C8-ceramide resulted in a nearly four-fold increase in endogenous forms of ceramide after 2 h. Other studies have demonstrated large increases in endogenous ceramides in Madin-Darby canine kidney cells treated with C8-ceramide [40] and in A549 human lung adenocarcinoma cells treated with C6-ceramide [41, 42]. There is substantial evidence that this increase in endogenous ceramides is due to remodeling of short chain ceramides through de-acylation to sphingosine by ceramidases, followed by reacylation with longer-chain fatty acids via the ceramide recycling pathway [35, 41–43]. There is evidence that growth inhibition and cell cycle arrest induced by exogenous C6-ceramide may be mediated by the increases in endogenous long-chain ceramides [42]. Ceramide functions are chain length dependent (e.g., C16:0; C24:0′ C24:1), which may ultimately decide the fate of cellular events such as apoptosis, proliferation, or cell cycle arrest [41].

One unexpected finding in BV-2 cells treated with C8-ceramide was the normalization of ceramide to near control levels by 24 h since the cultures did not undergo a media change. This prompted us to establish the stability of C8-ceramide in the culture media and also measure levels in the media from BV-2 cells after treatment with C8-ceramide (Table 4). Our data showed no decrease in C8-ceramide concentration over 24 h in culture media incubated at 37°C in the absence of cells, demonstrating stability of the analog. However, C8-ceramide levels in media from BV-2 cells declined rapidly and decreased to <1 μM by 24 h. The decrease in both culture media and cellular levels indicates near complete metabolism of the analog by the BV-2 cells by 24 h, without incorporation into

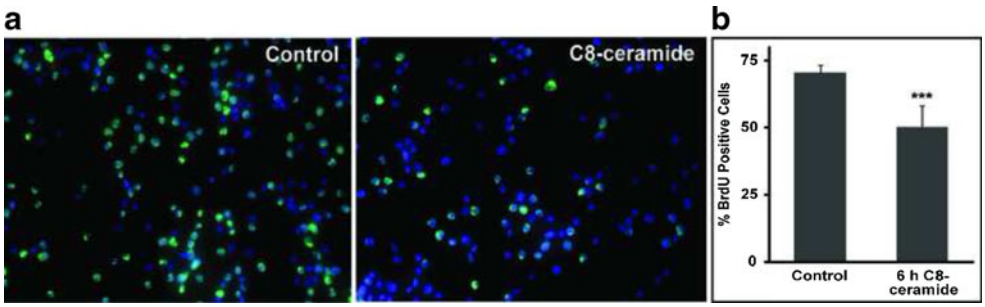

Fig. 7 Exogenous C8-ceramide inhibited BrdU incorporation in BV-2 cells. **a** Representative images of BrdU uptake in BV-2 controls and cells treated with exogenous C8-ceramide. Cells were plated in 96-well plates, allowed to attach overnight, and then treated with 30-μM C8-ceramide for 6 h. The media were then replaced with fresh media containing BrdU, and cells were incubated for 2 h. Cells were labeled with anti-BrdU antibody, followed by DAPI counterstaining, and imaged. *Blue* DAPI, *green* BrdU. Original magnification×200. **b** Quantification of BrdU-positive cells as a percentage of total cells. Two sets of images were captured from four wells each from controls and C8-ceramide treated. $^{***}p<0.001$ compared with controls by unpaired t-test. Note: Figs. 3 and 7 may appear black and white in print version

SM. While we did not examine the metabolism of exogenous C8-ceramide in BV-2 cells since the focus of these studies was the role of D609 in cell proliferation, our data indicate an additional factor to be considered in interpreting results from exogenous ceramide treatments. It has been noted that, since ceramides partition in membranes, the concentration of ceramide in relation to the number of cells is a significant factor influencing the outcome due to surface concentration effects, i.e., fewer cells treated with the same concentration of ceramide may respond differently than if the cell density is higher [36]. Our data indicate that in addition to surface concentration effects, metabolism of ceramide by the cells may be another factor since higher density cultures will metabolize a given amount of ceramide faster than low-density cultures, altering the overall response.

Recent studies showed that 2-hydroxyoleic acid (2OHOA) stimulates SMS and causes cell cycle arrest, cell differentiation, and autophagy or apoptosis in cancer cells [44]. Normal (non-tumor MRC-5) cells were unaffected by 2OHOA. Status of ceramide levels, as well as effect of D609 alone on these cell lines, was not presented. These effects may be specific to cell type and experimental conditions. Barcelo-Coblijn et al. [44] also have observed anti-proliferative effects for D609 (personal communication, Drs. Halver and Escriba PNAS 2011 paper corresponding authors of [44]). In these studies, 2OHOA increased SM levels>2.5 times in A549 and 5 times in U118 cells compared to controls, which may drastically affect the plasma membrane phospholipid composition/distribution. The source of ceramide needed for this large increase in SM synthesis was also unclear.

Our studies demonstrated reduction of cerebral infarct by D609 treatment in a rat stroke model and attributed the protection by D609 to cell cycle regulation [23]. After stroke, expression of cell cycle-related proteins is up-regulated. There is a dual effect to induction of the cell cycle. Proliferation of astrocytes and microglia contributes to glial scar formation and release of inflammatory factors [20]. Mature neurons are post-mitotic, yet apparently must continuously hold the cell cycle in check [45]. Failure of this cell cycle control in mature neurons results not in proliferation but cell death. Thus, inhibition of the cell cycle after stroke would attenuate astrocyte and microglia proliferation and also rescue neurons from cell death due to aberrant cell cycle induction. This is supported by studies demonstrating that administration of cell cycle inhibitors after ischemia dramatically reduced neuronal death [46].

Whether inflammatory responses after injury are harmful or helpful to recovery is a complex issue [47, 48]. TNF produced by microglia offered protection to neurons after ischemia [49]. Ablation of proliferating microglia resulted in an increase in the number of cells (unknown identity) expressing pro-inflammatory cytokines [50]. In the absence of activated microglia/macrophages, which cells are the source of pro-inflammatory cytokines is unclear? Defining the role of microglia/macrophages in CNS pathologies is a challenge since they are the source for both pro-inflammatory cytokines as well as neurotrophic factors [51]. Our current studies show that D609 inhibited proliferation of RAW 264.7 macrophages and three glia cells lines (BV-2 and N9 microglia, and DITNC$_1$ astrocytes) and thus may provide benefit after stroke by inhibiting proliferation of astrocytes and microglia. Another possibility is that D609 may prevent neuronal death by blocking aberrant induction of the cell cycle at the early reperfusion in mature neurons (24-h reperfusion); however, it may not interfere with proliferation of microglia/macrophages (72-h reperfusion) that are the source of trophic factors [52] during repair phase of stroke [23].

Acknowledgements Supported by NIH R01 NS063959 and AHA 11GRNT7360066 and resources provided by Veterans Affairs Hospital, Madison, WI. The authors have no conflict of interest to declare.

References

1. Adibhatla RM, Hatcher JF, Gusain A (2012) Tricyclodecan-9-yl-xanthogenate (D609) mechanism of actions: a mini-review of literature. Neurochem Res 37:671–679
2. Sauer G, Amtmann E, Melber K et al (1984) DNA and RNA virus species are inhibited by xanthates, a class of antiviral compounds with unique properties. Proc Natl Acad Sci 81:3263–3267
3. Sultana R, Newman SF, Abdul HM et al (2006) Protective effect of D609 against amyloid-β 1-42 induced oxidative modification of neuronal proteins: redox proteomics study. J Neurosci Res 84:409–417
4. Zhou DH, Lauderback CM, Yu T et al (2001) D609 inhibits ionizing radiation-induced oxidative damage by acting as a potent antioxidant. J Pharmacol Exp Ther 298:103–109
5. Amtmann E (1996) The antiviral, antitumoural xanthate D609 is a competitive inhibitor of phosphatidylcholine-specific phospholipase C. Drugs Exp Clin Res 22:287–294
6. Chen C, Hu Q, Yan J et al (2007) Multiple effects of 2ME2 and D609 on the cortical expression of HIF-1α and apoptotic genes in a middle cerebral artery occlusion induced focal ischemia rat model. J Neurochem 102:1831–1841
7. Monick MM, Carter AB, Gudmundsson G et al (1999) A phosphatidylcholine-specific phospholipase C regulates activation of p42/44 mitogen-activated protein kinases in lipopolysaccharide-stimulated human alveolar macrophages. J Immunol 162:3005–3012
8. Zhang F, Zhao G, Dong Z (2001) Phosphatidylcholine-specific phospholipase C and D in stimulation of RAW264.7 mouse macrophage-like cells by lipopolysaccharide. Intl Immunopharmacol 1:1375–1384
9. Machleidt T, Kramer B, Adam D et al (1996) Function of the p55 TNF receptor "death domain" mediated by phosphatidylcholine-specific PLC. J Exp Med 184:725–733
10. Zhang L, Zhao J, Su L et al (2010) D609 inhibits progression of preexisting atheroma and promotes lesion stability in apolipoprotein E-/- mice. A role of phosphatidylcholine-specific phospholipase in atherosclerosis. Arterioscler Thromb Vasc Biol 30:411–418

11. Larsen EC, Hatcher JF, Adibhatla RM (2007) Effect of tricyclodecan-9-yl potassium xanthate (D609) on phospholipid metabolism and cell death during oxygen-glucose deprivation in PC12 cells. Neuroscience 146:946–961
12. Yu ZF, Nikolova-Karakashian M, Zhou DH et al (2000) Pivotal role for acidic sphingomyelinase in cerebral ischemia-induced ceramide and cytokine production, and neuronal apoptosis. J Mol Neurosci 15:85–97
13. Ruvolo PP (2001) Ceramide regulates cellular homeostasis via diverse stress signaling pathways. Leukemia 15:1153–1160
14. Carrasco S, Merida I (2007) Diacylglycerol, when simplicity becomes complex. Trends Biochem Sci 32:27–36
15. Tafesse FG, Ternes P, Holthuis JCM (2006) The multigenic sphingomyelin synthase family. J Biol Chem 281:29421–29425
16. Huitema K, van den Dikkenberg J, Brouwers JFHM et al (2004) Identification of a family of animal sphingomyelin synthases. EMBO J 23:33–44
17. Luberto C, Hannun YA (1998) SM synthase, a potential regulator of intracellular levels of ceramide and diacylglycerol during SV40 transformation. Does SM synthase account for the putative PC-specific PLC? J Biol Chem 273:14550–14559
18. Luberto C, Yoo DS, Suidan HS et al (2000) Differential effects of sphingomyelin hydrolysis and resynthesis on the activation of NF-kappa B in normal and SV40-transformed human fibroblasts. J Biol Chem 275:14760–14766
19. Riboni L, Viani P, Bassi R et al (2001) Basic fibroblast growth factor-induced proliferation of primary astrocytes. Evidence for the involvement of sphingomyelin biosynthesis. J Biol Chem 276: 12797–12804
20. Byrnes KR, Faden AI (2007) Role of cell cycle proteins in CNS injury. Neurochem Res 32:1799–1807
21. Wang W, Bu B, Xie M et al (2009) Neural cell cycle dysregulation and central nervous system diseases. Prog Neurobiol 89:1–17
22. Ogretmen B, Hannun YA (2004) Biologically active sphingolipids in cancer pathogenesis and treatment. Nat Rev Cancer 4:604–616
23. Adibhatla RM, Hatcher JF (2010) Protection by D609 through cell-cycle regulation after stroke. Mol Neurobiol 41:206–217
24. Blasi E, Barluzzi R, Bocchini V et al (1990) Immortalization of murine microglial cells by a v-raf/v-myc carrying retrovirus. J Neuroimmunol 27:229–237
25. Righi M, Mori L, De Libero G et al (1989) Monokine production by microglial cell clones. Eur J Immunol 19:1443–1448
26. Raschke WC, Baird S, Ralph P et al (1978) Functional macrophage cell lines transformed by Abelson leukemia virus. Cell 15:261–267
27. Radany EH, Brenner M, Besnard F et al (1992) Directed establishment of rat brain cell lines with the phenotypic characteristics of type 1 astrocytes. Proc Natl Acad Sci 89:6467–6471
28. Lauderback CM, Drake J, Zhou D et al (2003) Derivatives of xanthic acid are novel antioxidants: application to synaptosomes. Free Radic Res 37:355–365
29. Bai A, Meier GP, Wang Y et al (2004) Prodrug modification increases potassium tricyclo[5.2.1.$0^{2,6}$]-decan-8-yl dithiocarbonate (D609) chemical stability and cytotoxicity against U937 leukemia cells. J Pharmacol Exp Ther 309:1051–1059
30. Furuya K, Ginis I, Takeda H et al (2001) Cell permeable exogenous ceramide reduces infarct size in spontaneously hypertensive rats supporting in vitro studies that have implicated ceramide in induction of tolerance to ischemia. J Cereb Blood Flow Metab 21:226–232
31. Yang NC, Jeng KC, Ho WM et al (2000) DHEA inhibits cell growth and induces apoptosis in BV-2 cells and the effects are inversely associated with glucose concentration in the medium. J Steroid Biochem Mol Biol 75:159–166
32. Wang N, Lv X, Su L et al (2006) D609 blocks cell survival and induces apoptosis in neural stem cells. Bioorg Med Chem Lett 16:4780–4783
33. Yakovlev AG, Faden AI (2001) Caspase-dependent apoptotic pathways in CNS injury. Mol Neurobiol 24:131–144
34. Chiba N, Masuda A, Yoshikai Y et al (2007) Ceramide inhibits LPS-induced production of IL-5, IL-10, and IL-13 from mast cells. J Cell Physiol 213:126–136
35. Bartke N, Hannun YA (2009) Bioactive sphingolipids: metabolism and function. J Lipid Res 50:S91–96
36. Luberto C, Kraveka JM, Hannun YA (2002) Ceramide regulation of apoptosis versus differentiation: a walk on a fine line. Lessons from neurobiology. Neurochem Res 27:609–617
37. Hannun YA, Obeid LM (2011) Many ceramides. J Biol Chem 286:27855–27862
38. Fukunaga T, Nagahama M, Hatsuzawa K et al (2000) Implication of sphingolipid metabolism in the stability of the Golgi apparatus. J Cell Sci 113(Pt 18):3299–3307
39. Lipsky NG, Pagano RE (1985) A vital stain for the Golgi apparatus. Science 228:745–747
40. Abe A, Wu D, Shayman JA et al (1992) Metabolic effects of short-chain ceramide and glucosylceramide on sphingolipids and protein kinase C. Eur J Biochem 210:765–773
41. Grosch S, Schiffmann S, Geisslinger G (2012) Chain length-specific properties of ceramides. Prog Lipid Res 51:50–62
42. Ogretmen B, Pettus BJ, Rossi MJ et al (2002) Biochemical mechanisms of the generation of endogenous long chain ceramide in response to exogenous short chain ceramide in the A549 human lung adenocarcinoma cell line. Role for endogenous ceramide in mediating the action of exogenous ceramide. J Biol Chem 277:12960–12969
43. Takeda S, Mitsutake S, Tsuji K et al (2006) Apoptosis occurs via the ceramide recycling pathway in human HaCaT keratinocytes. J Biochem 139:255–262
44. Barcelo-Coblijn G, Martin ML, de Almeida RF et al (2011) Sphingomyelin and sphingomyelin synthase (SMS) in the malignant transformation of glioma cells and in 2-hydroxyoleic acid therapy. Proc Natl Acad Sci 108:19569–19574
45. Herrup K, Yang Y (2007) Cell cycle regulation in the postmitotic neuron: oxymoron or new biology? Nat Rev Neurosci 8:368–378
46. Osuga H, Osuga S, Wang F et al (2000) Cyclin-dependent kinases as a therapeutic target for stroke. Proc Natl Acad Sci 97:10254–10259
47. Kriz J (2006) Inflammation in ischemic brain injury: timing is important. Crit Rev Neurobiol 18:145–157
48. Venero JL, Burguillos MA, Brundin P et al (2011) The executioners sing a new song: killer caspases activate microglia. Cell Death Differ 18:1679–1691
49. Lambertsen KL, Clausen BH, Babcock AA et al (2009) Microglia protect neurons against ischemia by synthesis of tumor necrosis factor. J Neurosci 29:1319–1330
50. Lalancette-Hebert M, Gowing G, Simard A et al (2007) Selective ablation of proliferating microglial cells exacerbates ischemic injury in the brain. J Neurosci 27:2596–2605
51. Ekdahl CT, Kokaia Z, Lindvall O (2009) Brain inflammation and adult neurogenesis: the dual role of microglia. Neuroscience 158:1021–1029
52. Madinier A, Bertrand N, Mossiat C et al (2009) Microglial involvement in neuroplastic changes following focal brain ischemia in rats. PLoS ONE 4:e8101
53. Day TW, Wu CH, Safa AR (2009) Etoposide induces protein kinase Cdelta- and caspase-3-dependent apoptosis in neuroblastoma cancer cells. Mol Pharmacol 76:632–640
54. Lee S, Suk K (2007) Heme oxygenase-1 mediates cytoprotective effects of immunostimulation in microglia. Biochem Pharmacol 74:723–729